*PMM U.S.S.R.*, Vol.49, No.2, pp. 247-251, 1985
Printed in Great Britain

0021-8928/85 $10.00+0.00
Pergamon Journals Ltd.

# SOME PROPERTIES OF THE MOTION OF AN ARTIFICIAL MOON SATELLITE NEAR THE LIBRATION POINT*

M.KH. KHASANOVA

Qualitative analysis has been used /1—4/ to study certain properties of the motion of moon satellites near the libration point $L_1$. The moon is regarded as a body with unequal principal central moments of inertia, rotating slowly with constant angular velocity $n$ about the minor principal central axis of inertia.

Consider the plane problem of the moiton of a moon satellite in its equatorial plane. The axes of a rectangular system of Cartesian coordinates coincide with the principal axes of the central ellipsoid of inertia. The expansion of the gravity force function will be given by the following formula /5/:

$$U = \frac{fM}{r} + \frac{f}{r^5}\left[(B + C - 2A)x^2 + (A + C - 2B)y^2\right] + \ldots, \quad r = (x^2 + y^2)^{1/2} \tag{1}$$

where $f$ is the gravitational constant, $M$ is the mass of the moon, $A, B, C$ are its principal central moments of inertia, and $r$ is the distance from the centre of the moon.

The equations of motion of an equatorial satellite have the form

$$x'' - 2ny' - n^2x = U_x', \quad y'' + 2nx' - n^2y = U_y'. \tag{2}$$

Let us introduce into expression (1) and equations (2) the small dimensionless parameter $\alpha$, writing

$$\frac{B - C - 2A}{MR^2} = \alpha\lambda, \quad \frac{A + C - 2B}{MR^2} = \alpha\mu$$

where $\lambda$ and $\mu$ are constants and $R$ is the mean equatorial radius of the moon.

Then the force function (1) will be represented by a series in powers of the small parameter $\alpha$. When $\alpha = 0$, the ellipsoid becomes a sphere and the motion of the satellite in the inertial coordinate system occurs along an unperturbed Keplerian orbit.

System (2) admists of the Jacobi integral ($h$ is the Jacobi constant)

$$x'^2 + y'^2 = n^2(x^2 + y^2) + 2\left[\frac{fM}{r} + \frac{fM\alpha R^2}{r^3}(\lambda x^2 + \mu y^2) + \ldots - h\right]. \tag{3}$$

The coordinates of the libration point are found from the conditions $\partial U/\partial x = \partial U/\partial y = 0$, which for small $\alpha$ yield

$$x_0 = \pm\left(a_0 + \frac{3fM\alpha R^2}{n^2a_0^4}\lambda + \ldots\right), \quad y_0 = 0$$
$$y_0 = \pm\left(a_0 - \frac{3fM\alpha R^2}{n^2a_0^4}\mu + \ldots\right), \quad x_0 = 0; \quad a_0 = \left(\frac{fM}{n^2}\right)^{1/3}. \tag{4}$$

Putting in (3) $x' = y' = 0$ we find the critical values $h_*$ of the Jacobi constant for small $\alpha$

$$h_{01} = \frac{3fM}{a_0} + \frac{2fM\alpha R^2}{a_0^3}\lambda, \quad h_{02} = \frac{3fM}{a_0} + \frac{2fM\alpha R^2}{a_0^3}\mu.$$

A qualitative study of the properties of motion of the moon's satellites in its equatorial plane was carried out using the following values of the astrodynamic constants /5/: $A = 0.8878\,1798 \cdot 10^{29}$ kg.km$^2$, $fM = 4.9024779 \cdot 10^{-6}$ km$^3$/sec$^2$, $B = 0.88800195 \cdot 10^{29}$ kg.km$^2$, $n = 2.661699989 \cdot 10^{-6}$ sec, $C = 0.88836978 \cdot 10^{29}$ kg.km$^2$ and $R = 1738.09$ km.

The above values yield $h_* = -0.1162 \cdot 10^{-3}$ km$^2$/sec$^2$.

When the height of the satellite above the moon's surface is varied from $H = 50$ km to 100 km in 10 km steps, the corresponding values of the Jacobi integral constant are $h \cdot 10^3 = -0.5137, -0.4104, -0.3121, -0.2100, -0.1162, +0.1900$ km$^2$/sec$^2$. The libration points $L_{2,3} = (\pm 0.9635; 0)$, $L_{4,5}$ $(0; \pm 0.8988)$ (at $H = 90$ km) are distributed symmetrically about the origin of coordinates.

Now, using the libration point $L_1$ as the origin of the new coordinate systems with the axes parallel to the axes of the old system, and making the change of variables $x = x_0 + \xi$ and $y = \eta$, we obtain the equations of motion of the satellite to terms of the to first-order of

*Prikl.Matem.Mekhan., 49, 2, 326-330, 1985

smallness in $\xi$ and $\eta$, in the form

$$\xi'' - 2n\eta' - d^2\xi = V_\xi' = \frac{\partial V}{\partial \xi} + \xi \frac{\partial^2 V}{\partial \xi^2} + \eta \frac{\partial^2 V}{\partial \xi \partial \eta} \tag{5}$$

$$\eta'' + 2n\xi' - n^2\eta = V_\eta' = \frac{\partial V}{\partial \eta} + \eta \frac{\partial^2 V}{\partial \eta^2} + \xi \frac{\partial^2 V}{\partial \eta \partial \xi}$$

$$V = \frac{fM}{\rho} + \frac{fM\alpha R^2}{\rho^3}[\lambda (x_0 + \xi)^2 + \mu\eta^2], \quad \rho^2 = (x_0 + \xi)^2 + \eta^2 .$$

The Jacobi integral is now transformed to

$$V^2 = \xi'^2 + \eta'^2 = n^2 (x_0^2 + \xi^2 + \eta^2 + 2x_0\xi) + 2 (\overline{V} + h) . \tag{6}$$

Assuming that $\xi$ and $\eta$ are sufficiently small and the value of the Jacobi constant $h$ is nearly critical, we shall study the properties of the motion of the satellite in the equatorial plane, and determine the types of singularities in the neighbourhood of the libration point $L_1$.

The approximate Hill curve /6/ in this case, up to second-order terms in $\xi$ and $\eta$, takes the form of an ellipse with eccentricity $\approx 0.50$

$$\frac{\xi^2}{a^2} + \frac{\eta^2}{b^2} = 1; \quad a = \sqrt{\frac{N_3}{N_1}}, \quad b = \sqrt{\frac{N_3}{N_2}},$$

$$N_1 = \frac{3n^2 + 12n^{10/3} fMR^2}{fM^{1/3}} \alpha\mu; \quad N_2 = \frac{n^{10/3} fMR^2\alpha (2\lambda - 5\mu)}{fM^{1/3}}$$

$$N_3 = 2 (h - n^{10/3} fM^{1/3} + n^2 fM\alpha R^2\mu) .$$

In the case when

$$x_0 = \pm\left(a_0 + \frac{3fM\alpha R^2}{n^2 a_0^4} \lambda + \ldots\right)$$

the characteristic equation of system (5) will become

$$\gamma^4 + \left(1 - \frac{4\lambda + 2\mu}{a_0^5}\right)\gamma^2 + 6\left(\frac{\mu - \lambda}{a_0^5}\right) = 0 .$$

When $\lambda > \mu$. Eq. (7) has two real roots and two purely imaginary conjugate roots. The parameters $|\lambda|^{1/3}$ and $|\mu|^{1/3}$ are constant quantities and depend on the moments of inertia and the mass of the body. The roots have the following form up to terms of the second-order of smallness with resepct to $\xi$ and $\eta$:

$$\gamma_{1,2} = \pm\sqrt{6|\lambda - \mu|}/a_0^4, \quad \gamma_{3,4} = \pm i.$$

When $\lambda < \mu$. Eq. (7) has two different, pairwise conjugate, purely imaginary roots

$$\gamma_{1,2} = \pm i\sqrt{6|\lambda - \mu|}/a_0^4, \quad \gamma_{3,4} = \pm i .$$

Therefore the libration point $L_1$ is a centre-type singularity only to a first approximation.

Using the system of concentric circles

$$\xi^2 + \eta^2 = d^2 \tag{8}$$

as the one-parameter family of curves /7/, we shall study the behaviour of the satellite trajectories around the libration point $L_1$ for various values of $h$ differing little from its critical value.

For every fixed value of $h$ there exists in the $\xi, \eta$-plane a curve $v^0(h)$ of zero velocities whose equation in polar coordinates has the following form after changing the old coordinates:

$$v^0(h) = n^2\rho^5 + 2h\rho^3 + 2fM\rho^2 + fMR^2 [(2C - B - A) + 3(B - A)\cos 2\varphi] = 0. \tag{9}$$

$$(\rho^2 = \xi^2 + \eta^2, \ \operatorname{arctg}\varphi = \eta/\xi) .$$

If the roots of (9) are real, then the Hill curve will divide the $\rho, \varphi$-plane into two regions: in one of them $v^2 < 0$ and no motion is possible, in the other $v^2 > 0$ and motion is possible and all trajectories corresponding to the given value of the Jacobi constant $h$ (Fig. 1, curves *1—4*) lie within it.

We note that Figs.1—3 are constructed for the case when $h = 0.4104 \cdot 10^{-3}$.

In determining the roots of (9) for the specific values of $h$, we note that:

1°. When $h > h_*$, the Hill curve is of no interest since the satellite may move away from the libration point $L_1$ without limit.

2°. When $h < h_*$, the Hill curve will be represented by a closed, oval-like curve surrounding the point $L_1$; motion is impossible inside it since $v^2 < 0$ (Fig.1, the dashed lines, Fig.2). Outside the oval $v^2 > 0$, and therefore a motion is possible (Fig.1, curves *1—4*, Figs.2, 3).

3°. When $h = -0.5136 \cdot 10^{-3}$, $-0.4104 \cdot 10^{-3}$, $-0.3121 \cdot 10^{-3}$ km$^2$/sec$^2$, the Hill curves surrounding $L_1$ have the form of ovals stretched along the ordinate. When $h$ with negative sign increase in modulus, the curves become less stretched and more circular.

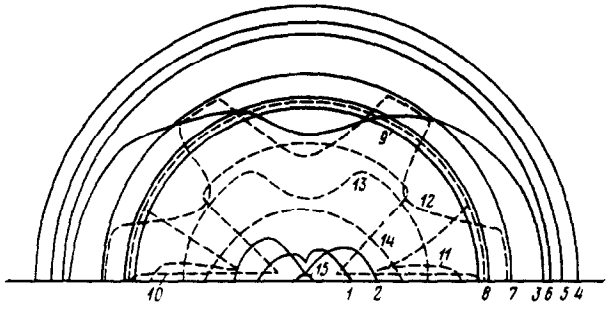


Fig.1

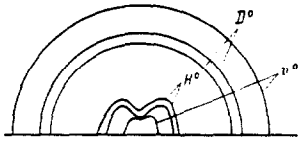


Fig.2

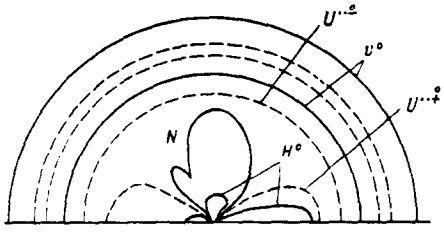


Fig.3

4°. For small values of $h$ ($|h| < 0.2100 \cdot 10^{-3}$ km$^2$/sec$^2$) the Hill curve takes a form resembling a lemniscate, and this implies the presence of centre-type singularities (Fig.1, curves *1*, *2*).

5°. When $h = h_*$, the inner curces contracts to the libration point $L_1$. We will study the bundle of trajectories emerging from a single point (elliptic when $D^\circ(h) < 0$, hyperbolic when $D^\circ(h) > 0$ and parabolic when $D^\circ(h) = 0$), by considering the Darwin curve whose equation in explicit form is /4, 6/

$$D^\circ(h) = 64\, n^4\rho^{10} + 124\, n^2 h\rho^8 + 124\, n^2 fM\rho^7 + 64\, n^2 fMR^2 [2C - B - A + (B - A)\cos 2\varphi]\,\rho^5 + 8f^2M^2\rho^4 + 24f^2M^2R^2 [2C - A - B + 3\,(B - A)\cos 2\varphi]\,\rho^2 + f^2M^2R^4 [(B + C - 2A)^2 + (A + C - 2B)^2]\,(39 + 53\cos 2\varphi + 21\cos 4\varphi) = 0. \quad (10)$$

Computing the roots of Eq.(10) for the values of $h$ used, we conclude that 1°. For all values of $h$ not exceeding the critical value $h_*$, the Darwin curves surrounding the point $L_1$ are nearly circular (Fig.1, curves *5*, *6*, *15*, and Fig.2).

2°. The Darwin curve has not discontinuities; from 1° it follows that when $h \neq h_*$ neither can it have branches moving to infinity; hence it must consist of closed loops.

3°. When $h = h_*$, the Darwin curve, as well as the Hill curve degenerate into the libration point $L_1$.

4°. For large values of $|h|$ a Darwin curve surrounds the libration point $L_1$. It is nearly circular and lies completely within the domain of possible motions (Fig.1, curves *5*, *15*). Within the curve (Fig.1, curves *5*, *15*) the characteristic $D^\circ(h) < 0$ and the bundle is elliptic, while outside it $D^\circ(h) > 0$ and the bundle is hyperbolic.

5°. When the values of $|h|$ increase, the circle-like Darwin regions where the trajectories are elliptic decrease, as well as the outer Hill curves.

Comparing the sets of the Hill and Darwin curves we come to the following conclusion. For low values of $h$, for which the Hill and Darwin curves were studied, different from $h_*$ corresponding to the libration point $L_1$, the Hill curve does not intersect the Darwin curve and is situated on the side of the Darwin curve on which the Darwin characteristic is positive and the bundle hyperbolic.

To carry out a more complete study of the qualitative pattern of motions of a satellite in a gravitational field of a triaxial ellipsoid, we shall consider the geometric locus of the contact between the trajectories and the topographic family of circles (8).

The equation of the geometric locus of contact (the contact characteristic) has the form

$$q^{\circ\circ}(h) = 2n^6\rho^{10} - 4n^4h\rho^8 - fMn^4R^2 [2(C - A) - B + (3B - 2A)\cos 2\varphi] \times \rho^5 \pm 2\{2n^4\rho^6 - 4n^2h\rho^4 - 2fMR^2n^3\rho^3 + 3n^2h^2R^2\rho^2 + \quad (11)$$

$$fM\left\{n^2R^2\left[2\left(C-A\right)-B+\left(3B-2A\right)\cos 2\varphi\right]+\frac{3h}{n^2R^2}\right\}\rho-3f^2M^2\Big\}=0\,.$$

Using curve (11) and the results in /4/ we shall study the following curves a) $q^{\circ\circ\circ}(h)=0$, i.e. a geometric locus of contact with the same circles (8) for the forward-motion trajectories; b) $q^{\circ\circ\circ}(h)=0$ i.e., the geometric locus of contact with the same circles for the reverse-motion trajectories.

The curve a) divides the whole $\rho, q$ plane into a region of purely external contacts between the forward-motion trajectories and the circles (8) $q^{\circ\circ\circ}(h)$ and the region of purely internal contacts of the forward trajectories $q^{\circ\circ\pm}(h)$. Curve b) divides the plane into a region of purely external contacts between the reverse motion trajectories and the circles (8) $q^{\circ\circ\mp}(h)$, and the region of purely internal contacts between the reverse motion trajectories and the circles (8) $q^{\circ\circ\mp}(h)$. The curves $q^{\circ\circ+}$ represents the region of mixed contacts in which both internal and external contacts are possible. Curves *7—9* in Fig.1 depict the boundaries of the region of purely external contacts of the forward-motion trajectories; the curves *10—12* (dashed lines) represent the boundaries of the region of purely internal contacts of the forward-motion trajectories. A boundary of the region of purely external contacts of the reverse motion trajectories (not shown in Fig.1) passes between curves *3* and *7*, *3* and *6*. Curve *13* and the curves lying between curves *2* and *13*, *13* and *8*, represent the boundary of the region of purely internal contacts of the reverse-motion trajectories.

When $h=h_*$, the critical value of the contact characteristic degenerates into the libration point $L_1$. When the values of $|h|$ increase further the regions of external and internal contact of the trajectories of (forward and reverse) motion do not come in contact with each other.

The internal part of the geometric locus of contacts represents a Hadamard curve (the contact within the Hadamard curve will be external for any possible trajectories) whose equation has the form

$$H^{\circ}(q)=2n^2\rho^2-fM\rho^3-2fMR^2\left[(A-B+2C)-3\left(A-B\right)\cos 2q\right]=0\,.$$

In the case in question the curve $H^{\circ}(q)$ resembles a lemniscate Figs.2, 3).

We will now carry out a short analysis of certain general properties of the contact characteristic with the level lines

$$U(x,\ y)=-h=\text{const}\,. \tag{12}$$

Using system (2) and the Jacobi integral (3), we shall write the equation of the geometric locus of contacts of the trajectories with the level lines (12) in the form

$$2N(U-h)=2nE^{\circ}\left[2(U-h)^2-E^2\right]=0 \tag{13}$$
$$(E^2=U_x^{\circ 2}+U_y^{\circ 2},\ N=U_{xx}^{\circ}U_y^{\circ 2}-2U_{xy}^{\circ}U_x^{\circ}U_y^{\circ}+U_{yy}^{\circ}U_x^{\circ 2})\,.$$

We write the equation of the Hadamard curve as follows:

$$H^{\circ}(U)=(n^2E-N)E=0\,.$$

Let us inspect curve (13) for the value of $h=-0.4104\cdot 10^{-3}$ km$^2$/sec$^2$ and of the curves a) $q^{\circ\circ\circ}(h)$ and b) $q^{\circ\circ\mp}(h)$ (Fig.1, curves *7—12* and Fig.3). We shall utilize the curves $E^{\circ}(U)$ and $N^{\circ}(U)$ (in the present case the curve $E^{\circ}(U)$ degenerates into the libration point $L_1$).

The Hadamard curves $H^{\circ}(U)$ and the curves of the geometric locus of contact between the trajectories (13), i.e. $U^{\circ\circ\circ}(h)$ and the level lines (1) pass outside the curve $N^{\circ}(U)$. The geometric locus of contact $U^{\circ\circ+}(h)$ lies inside the Hadamard curve $H^{\circ}(U)$. On the other hand, the curve $N^{\circ}(U)$ passes through the libration point $L_1$ and has a common tangent with the Hadamard curve and the curve $U^{\circ\circ+}(h)$.

For large values of $h$ the curve $U^{\circ\circ\circ}$ consists of ring-like regions enveloping the inner and outer Hill regions. When $h=h_*$, the geometric locus of the tangents $U^{\circ\circ\circ}(h)$ degenerates into the libration point $L_1$. When $h=-0.4104\cdot 10^{-3}$ km$^2$/sec$^2$, lemniscate-like $U^{\circ\circ\mp}(h)$ branches of the geometric locus of contacts between the trajectories emerge from the libration point $L_1$ in both directions. A mixed type region $U^{\circ\circ\pm}(h)$ is situated between $U^{\circ\circ\circ}(h)$ and $U^{\circ\circ-}(h)$ (Fig.3).

The region $U^{\circ\circ+}(h)$ within which the libration point $L_1$ lies, represents the region of external contacts between the trajectories and level lines, i.e. a purely pericentric region.

The region $U^{\circ\circ-}(h)$, which is circular and embraces the mixed-type region $U^{\circ\circ\pm}(h)$ and libration point $L_1$, represent a region of purely internal contacts between the trajectories and level lines, i.e. a purely apocentric region.

The region of mixed types $U^{\circ\circ\pm}(h)$ is a pericentric region $U^{\circ\circ+}(h)$ and an apocentric region $U^{\circ\circ-}(h)$.

From Figs.1-3 it is clear that the higher thelevel of flight above the moon's surface (with an absolute value of $h$ exceeding the critical value), the greater the Hill region and the Darwin curves become smaller.

REFERENCES

1. KHASANOVA M.KH., Qualitative study of the properties of motion of a satellite of a spheroidal planet. PMM Vol.41, No.3, 1977.
2. KHASANOVA M.KH., On a form of the equations of motion of an equatorial satellite of a planet. Dokl. Akad. Nauk TadzhSSR, Vol.20, No.5, 1977.
3. KHASANOVA M.KH., On the regions of possible motion of the Jupiter and Saturn satellites. Dokl. Akad. Nauk TadzhSSR, Vol.20, No.8, 1977.
4. IBRAGIMOVA KH.B. and KHASANOVA M.KH., Qualitative properties of the motion of stars at the periphery of the galaxy. Pis'ma v Astron. zh. Vol.6, No.7, 1980.
5. ABALAKIN V.K., AKSENOV E.P., GREBENIKOV E.A. and RYABOV YU.A., Handbook of Celestial Mechanics and Astrodynamics. Moscow, Nauka, 1976.
6. MOISEYEV N.D., On certain general methods of studying the forms of motion on the problems of celestial mechanics. Tr. Gos. astron. in-ta im. P.K. Shternberg., Vol.7, No.1, 1936.
7. DEMIN V.G., Motion of an ARtificial Satellite in a Non-central Gravity Field. Moscow, Nauka, 1968.

Translated by L.K.

*PMM U.S.S.R.*, Vol.49, No.2, pp.251-254, 1985
Printed in Great Britain

0021-8928/85 $10.00+0.00
Pergamon Journals Ltd.

# ON THE ISOLATED CHARACTER OF SOLUTIONS WITH A STRONG ATTACHED SHOCK WAVE AT THE EDGES OF A v-SHAPED WING AND WEDGE*

A.V. GRISHIN

The transonic approximation is used to study the conical problems of supersonic flow past an infinite wedge and a *V*-shaped wing, the flow behind the attached shock wave is subsonic. The possibility of the existence of a flow with a strong shock in a plane perpendicular to the edge of the wing or wedge is clarified. For this reason the linear theory is used to study the boundary value problems for the perturbations in exact solutions with a plane shock. It is shown that the boundary value problems have a solution, provided that the plane shock wave corresponding to the exact solution is weak (in a plane perpendicular to the edge), and have no solution when the shock is strong.

Earlier /1/, the problem of flow past a *V*-shaped wing was studied, where the flow was supersonic behind the attached shock wave. Experimental investigations /2—4/ of the flow past a *V*-shaped wing resembling flows with a strong plane shock, made it possible to establish /4/ the isolated nature of the flow with a strong shock. Numerical methods /5/ and experimental methods /2—4/ were used to show that when the angle of attach of the *V*-shaped wing with a strong plane shock is reduced, a flow results with Mach interaction between the shock waves and the weak discontinuity at the edge. It was established /4/ that increasing the angle of attack causes detachment of the shock wave. A non-steady model of supersonic flow past an infinite wedge is proposed in /6/** (**see also Rusanov V.V. and Sharakshane A.A. Non-steady models of flow past conical bodies. Preprint In-ta prikl. matem. Akad. Nauk SSSR, Moscow, No.27, 1978, and Rusanov V.V. and Sharakshane A.A., Study of a linearized non-stationary model of flow past an infinite wedge. Preprint In-ta prikl. matem. Akad. Nauk SSSR, Moscow, No.103, 1980) and it is shown that a flow with a strong shock wave is unstable in this model. The non-existence of a flow with a strong shock represents a basically different case of a finite wedge and was proved using the hodograph method /7/ without taking into account the vorticity (in the transonic approximation). The result is generalized in /8/ to the case of vortical flows.

1. Assuming that the velocities are normalized with respect to the speed of sound, we shall consider the problems in the transonic approximation. We take, as the unperturbed flow, the uniform flow past a wedge with a strong or weak shock wave attached to the edge of the wedge, in the case when the flow behind the shock is subsonic. We choose a coordinate system attached to the edge of the wedge, in which the $z$ axis is directed along the edge and the $x$ axis along the velocity vector behind the shock wave (Fig.1). The transonic velocity components $\mathbf{v} = (1 + u, v, w)$ can then be represented in the form $u = u_{01}, v = v_{01}, w = 0$ in front of the wave,

*Prikl.Matem.Mekhan., 49, 2, 330-334, 1985